

Bimodal growth of Fe islands on graphene

Yi-Sheng Gu(顾翊晟), Qiao-Yan Yu(俞俏滟), Dang Liu(刘荡), Ji-Ce Sun(孙蓟策), Rui-Jun Xi(席瑞骏), Xing-Sen Chen(陈星森), Sha-Sha Xue(薛莎莎), Yi Zhang(章毅), Xian Du(杜宪), Xu-Hui Ning(宁旭辉), Hao Yang(杨浩), Dan-Dan Guan(管丹丹), Xiao-Xue Liu(刘晓雪), Liang Liu(刘亮), Yao-Yi Li(李耀义), Shi-Yong Wang(王世勇), Can-Hua Liu(刘灿华), Hao Zheng(郑浩), and Jin-Feng Jia(贾金锋),

Citation: Chin. Phys. B, 2024, 33 (**6**): 068104. DOI: 10.1088/1674-1056/ad322f
Journal homepage: http://cpb.iphy.ac.cn; http://iopscience.iop.org/cpb

What follows is a list of articles you may be interested in

Effect of external magnetic field on the instability of THz plasma waves in nanoscale graphene field-effect transistors

Liping Zhang(张丽萍), Zongyao Sun(孙宗耀), Jiani Li(李佳妮), and Junyan Su(苏俊燕)
Chin. Phys. B, 2024, 33 (**4**): 048102. DOI: 10.1088/1674-1056/ad1e66

Intercalation of hafnium oxide between epitaxially-grown monolayer graphene and Ir(111) substrate

Yi Biao(表奕), Hong-Liang Lu(路红亮), Hao Peng(彭浩), Zhi-Peng Song(宋志朋), Hui Guo(郭辉), and Xiao Lin(林晓)
Chin. Phys. B, 2023, 32 (**9**): 098102. DOI: 10.1088/1674-1056/accff4

Morphological features and nanostructures generated during SiC graphitization process

Wen-Xia Kong(孔雯霞), Yong Duan(端勇), Jin-Zhe Zhang(章晋哲),Jian-Xin Wang(王剑心), and Qun Cai(蔡群)
Chin. Phys. B, 2023, 32 (**6**): 068103. DOI: 10.1088/1674-1056/acb766

Longitudinal conductivity in ABC-stacked trilayer graphene under irradiating of linearly polarized light

Guo-Bao Zhu(朱国宝), Hui-Min Yang(杨慧敏), and Jie Yang(杨杰)
Chin. Phys. B, 2022, 31 (**8**): 088102. DOI: 10.1088/1674-1056/ac7205

Thermoelectric characteristics of flexible reduced graphene oxide/silver selenide nanowire composites prepared by a facile vacuum filtration process

Zuo Xiao(肖佐), Yong Du(杜永), Qiufeng Meng(孟秋风), and Lei Wang(王磊)
Chin. Phys. B, 2022, 31 (**2**): 028103. DOI: 10.1088/1674-1056/ac447e

---

Bimodal growth of Fe islands on graphene

Yi-Sheng Gu(顾翊晟)[1], Qiao-Yan Yu(俞俏滟)[1], Dang Liu(刘荡)[1], Ji-Ce Sun(孙蓟策)[1], Rui-Jun Xi(席瑞骏)[1], Xing-Sen Chen(陈星森)[1], Sha-Sha Xue(薛莎莎)[1], Yi Zhang(章毅)[1], Xian Du(杜宪)[1], Xu-Hui Ning(宁旭辉)[1], Hao Yang(杨浩)[1], Dan-Dan Guan(管丹丹)[1], Xiao-Xue Liu(刘晓雪)[1], Liang Liu(刘亮)[1], Yao-Yi Li(李耀义)[1], Shi-Yong Wang(王世勇)[1], Can-Hua Liu(刘灿华)[1], Hao Zheng(郑浩)[1,†], and Jin-Feng Jia(贾金锋)[1,2,3,‡]

[1] *Key Laboratory of Artificial Structures and Quantum Control (Ministry of Education), TD Lee Institute, Shenyang National Laboratory for Materials Science, School of Physics and Astronomy, Shanghai Jiao Tong University, Shanghai* 200240, *China*

[2] *Department of Physics, Southern University of Science and Technology, Shenzhen* 518055, *China*

[3] *Quantum Science Center of Guangdong–Hong Kong–Macao Greater Bay Area (Guangdong), Shenzhen* 518045, *China*

(Received 18 February 2024; revised manuscript received 8 March 2024; accepted manuscript online 11 March 2024)

Magnetic metals deposited on graphene hold the key to applications in spintronics. Here, we present the results of Fe islands grown on graphene/SiC(0001) by molecular beam epitaxy, which are investigated by scanning tunneling microscopy. The two types of islands distinguished by flat or round tops are revealed, indicating bimodal growth of Fe. The atomic structures on the top surfaces of flat islands are also clearly resolved. Our results may improve the understanding of the mechanisms of metals deposited on graphene and pave the way for future spintronic applications of Fe/graphene systems.

Keywords: graphene, magnetism, molecular beam epitaxy, scanning tunneling microscopy

PACS: 81.15.Hi, 73.20.–r **DOI:** 10.1088/1674-1056/ad322f

1. Introduction

Since the discovery of graphene overturned the argument that monolayer or two-dimensional (2D) materials are unstable and could not exist,[1–4] it has aroused significant interest. The most fascinating property of graphene is its massless Dirac dispersion of low-energy excitation,[5–8] which leads to novel phenomena such as the half integer quantum Hall effect (QHE) under an external magnetic field even at room temperature.[9–12] Recently, the properties of multilayer graphene with moiré superlattices have become a hot topic due to their strong correlation and possible topological order.[13] Other than pristine graphene, the hybrid systems of graphene and other materials may generate new possibilities.[14] One example is that properly doped graphene is theoretically predicted to possess $d+id$ superconductivity due to repulsive interactions.[15–17] This superconductivity has been experimentally demonstrated in Ca-intercalated bilayer graphene.[18–20] Furthermore, after building heterostructure between graphene and other functional materials, graphene may gain certain properties directly from the deposited material without breaking intrinsic electronic states. These heterostructures hold many feasible applications. In particular, with promising applications in spintronics and memory devices, magnetic metal/graphene heterostructures are of great interest.[21–23]

Studies of magnetic metal/graphene heterostructure mainly focus on realizing stronger magnetic properties in comparison to pristine magnetic materials. One example is that Baltic *et al.* discovered that the superlattice of Dy atoms on graphene has great magnetic stability due to the 6-fold symmetry of the absorption site, as well as the electron/phonon properties of graphene.[25] Another case investigated by Ren *et al.*, shows that graphene/Ru substrate acts as a medium to support Ruderman–Kittel– Kasuya–Yosida (RKKY) indirect spin exchange for Mn trimers.[26] With regard to ferromagnetic materials, Gao *et al.* found that when Ni nano-islands are grown on graphene, the graphene becomes spin polarized due to the antiferromagnetic coupling between Ni nano-islands and graphene.[27] Moreover, many researchers reported that adatoms or islands of Fe, the most typical magnetic material, when grown on graphene, demonstrates the complexity of both growth morphology and electronic states in such heterostructure.[28–33] Although there have been many advances in the study of Fe/graphene structures, the most challenging issue of this heterostructure, as with most other metal/graphene systems, is the three-dimensional (3D) growth of Fe, which usually takes irregular island shapes and small island sizes.[23,29–32,35] Therefore, the preparation of Fe islands on graphene with better morphology is desirable.

On the other hand, scanning tunneling microscopy/spectroscopy (STM/S) is a powerful technique to characterize electronic properties of single crystals on atomic scale.[36–41] More importantly, the combination of material growth techniques, especially molecular beam epitaxy (MBE)

[†]Corresponding author. E-mail: haozheng1@sjtu.edu.cn
[‡]Corresponding author. E-mail: JfJia@sjtu.edu.cn

© 2024 Chinese Physical Society and IOP Publishing Ltd

and STM/S, allows us to obtain high-quality thin films of target samples (on certain substrates in some cases) and immediately acquire the real space morphology and electronic properties of the samples. This combination has already played an important role in the study of functional heterostructures, epitaxial 2D materials, novel quantum materials, interface or thin-film superconductivity, quasiparticle interference, etc.[42–60] In this article, we take advantage of the combination of MBE and STM to further examine and control the growth morphology and electronic states of Fe on graphene/SiC(0001).

2. Methods

Our graphene substrates were obtained in ultrahigh vacuum (UHV), where the basic pressure is at approximately 2×10^{-10} Torr, by annealing of 6H-SiC(0001) at 1450 °C for 20 min. The pressure did not exceed 2×10^{-8} Torr during the annealing process, and dropped back below 3×10^{-10} after annealing. Fe was then deposited on graphene by electron beam evaporation, while the substrate was kept at room temperature. After the samples were further grown and annealed at various temperatures and cooled down to room temperature, they were immediately transferred to a commercial STM, which is also at UHV, for measurement. The STM measurement in this article was carried out at liquid helium temperature (4.7 K). The STM tips are made from electrochemically etched tungsten wire.

3. Results

Figure 1 demonstrates the different topographies of the samples with various Fe coverages and sample annealing temperatures. Bilayer graphene on 6H-SiC(0001) without any Fe deposition is shown in Fig. 1(a). The inset is an STM image with atomic resolution, displaying typical honeycomb structure of graphene. The STM image serves as proof that graphene surface is atomically clean. Then, as illustrated in Fig. 1(b), about 8.6 monolayer (ML) Fe was deposited on graphene, while the substrate was kept at room temperature. Fe forms small rounded clusters with short inter-cluster distance. In contrast, the morphology of 12.5 ML Fe on graphene annealed at 873 K, as displayed in Fig. 1(c), shows that the configuration of Fe exhibits a transition from high-density clusters to low-density crystalline islands during annealing. Moreover, with larger Fe coverage and higher annealing temperature, the size of the Fe islands and distance between neighboring Fe islands further increase. This formation of Fe islands is dominated by a thermodynamic process. Figure 1(d) shows the result of 37.2 ML Fe deposited on graphene at 873 K with subsequent annealing at 973 K, in which well-defined shaped Fe islands are established.

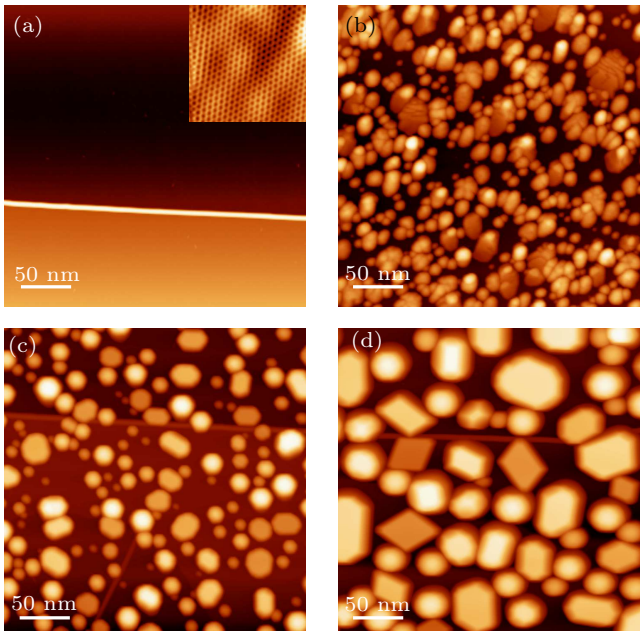


Fig. 1. STM images of the Fe/graphene with different Fe coverages and growth/annealing temperatures. (a) Topography of epitaxial graphene on SiC. The figure at top right is a 5 nm×5 nm STM image with atomic resolution. (b) 8.6 ML Fe deposited with substrate at room temperature. (c) 12.5 ML Fe deposited at substrate room temperature and annealed at 873 K for 15 min. (d) 37.2 ML Fe deposited at 873 K and annealed at 973 K for 15 min.

4. Discussion

Having acquired better Fe island shapes in the Fe/graphene system, we next pay attention to the general properties of Fe islands. Figure 2(a) shows the 3D view of Fe islands on graphene. One may find that the morphology of various Fe islands can be divided into two categories. One is islands with nearly perpendicular cliffs with large plateaus on the top, while the other is islands with round tops (the pyramids with much smaller plateaus on the top are also considered as Fe islands with round tops). With these two categories in mind, we subsequently count the height of the Fe islands with different shapes, as shown in the histograms in Fig. 2(b). The ratio of the number of Fe islands with flat tops to the Fe islands with round tops is about 1:2. The average height of islands with flat tops is 15.16 nm, lower than the 17.78 nm of round-top islands. These differences are also evident by looking at the orange and green curves that present the fittings of the histograms with Gaussian distribution.

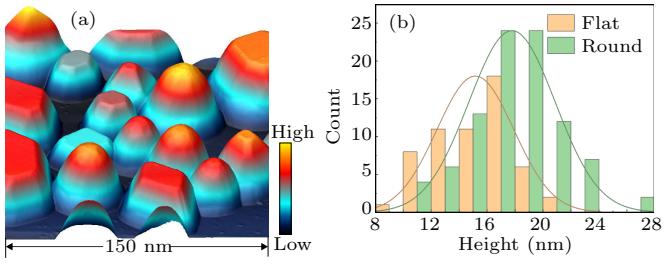


Fig. 2. Fe islands with various shapes. (a) 3D view of an 150 nm×150 nm area showing the different shapes of Fe islands. The islands can be divided into two types based on flat or round tops. (b) The orange (green) histograms display the distribution of heights of Fe islands with flat (round) tops. The orange (green) curves are the corresponding Gaussian fittings.

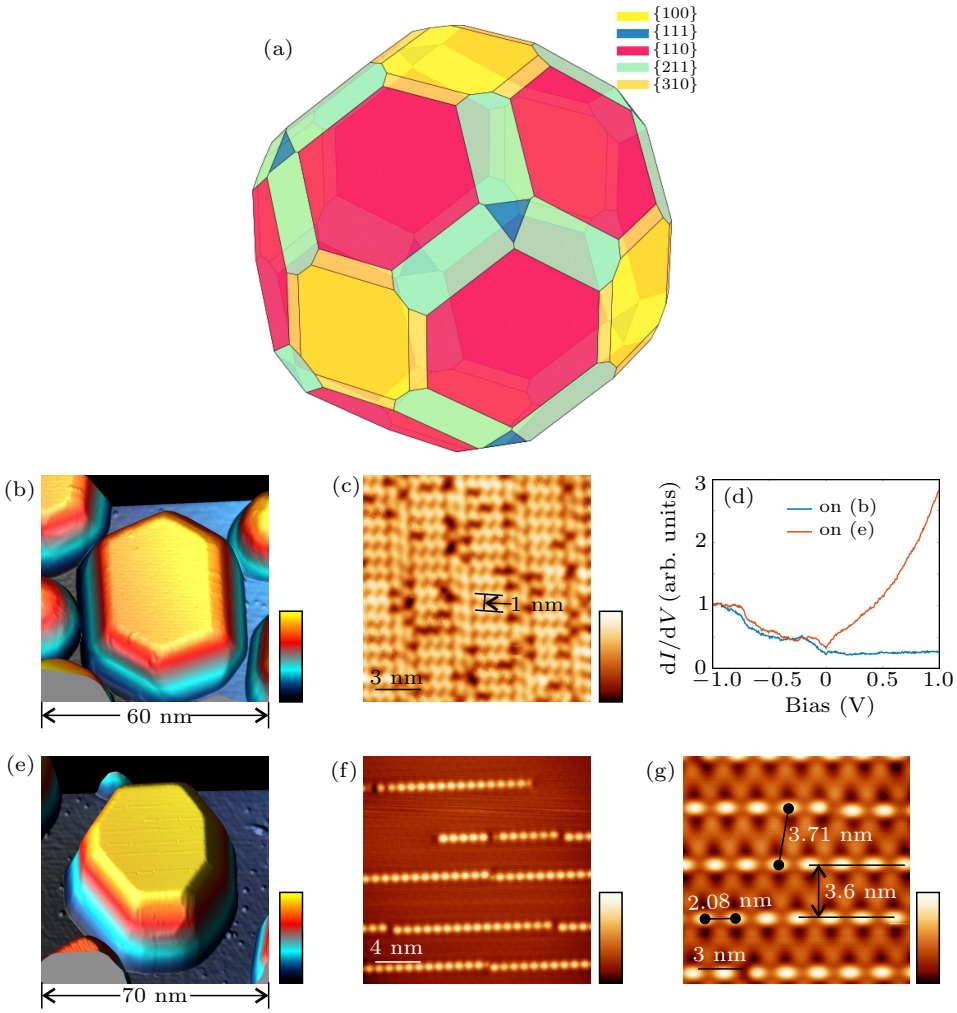


Fig. 3. Characterization of the island structures. (a) Wulff construction of bcc Fe. (b) 3D view of STM image of an island with flat (110) top facet. (c) STM image zoomed in at the top of the central island in (b). (d) $\mathrm{d}I/\mathrm{d}V$ spectra taken on the central islands in (b) (blue curve) and (e) (orange curve). (e) STM image of an island with (100) top surface. (f) STM image zoomed in at the top of the central island in (e). (g) 15 nm×15 nm STM image.

After checking the general shapes of the Fe islands, we turn to studying the specific shapes and electronic states on the tops of the islands with a flat top. Figure 3(a) is the result of Wulff construction of body centered cubic (bcc) Fe generated by Python Wulffpack.[61] Based on calculated results of surface energies of bcc Fe, we know that (110) and (100) surfaces have the lowest and second lowest surface energies.[62–64,64–68] (The surface energies chosen here to obtain the Wulff construction were calculated by Błoński and Kiejna.[65]) One can thus expect that once one has a crystalline Fe island, its facets will be dominated by (110) and (100) orientations. Moreover, the results in Fig. 3(a) shows that the shapes of (110) facets and (100) facets are hexagons and octagons, respectively. The Wulff construction with different facet shapes helps us to identify different facet orientations on our Fe islands with flat tops. Indeed, our STM images in Figs. 3(b) and 3(e) revealed the Fe islands with flat tops displayed in 3D view. The islands of interest are the ones located at the center of each image. Based on the direct comparison to the Wulff construction of Fig. 3(a), we believe that the top surface of the island in Fig. 3(b) is (110) surface, and that of Fig. 3(e) is (100) surface. We then measure the differential conductance ($\mathrm{d}I/\mathrm{d}V$) on different samples to reveal their local density of states (LDOS). In Fig. 3(d), the blue and orange curves correspond to the $\mathrm{d}I/\mathrm{d}V$ spectra taken on the (110) and (100) top facets of the central Fe island in Figs. 3(e) and 3(d), respectively. The LDOS on the two kinds of facets appear similarly in the occupied state, i.e., bias < 0, but differently in the empty state (bias > 0). In the empty state with bias voltage ranging from 0 V to 1 V, the LDOS intensity in the (100) facet increased with rising voltage, but the (110) LDOS remains constant.

Figure 3(c) is the STM image with atomic resolution on the top of the (110) facet in Fig. 3(b); instead of a well-ordered atomic arrangement, we only find nearly disordered stripes with an inter-stripe distance of approximately 1 nm. Figure 3(f) is the small-range STM image taken on the top of the (100) facet from the island in Fig. 3(e), which shows ordered stripes together with some disrupted bright dot arrays. Figure 3(g) is the STM image on the top of another island also with the (100) facet, which demonstrates much more ordered

patterns. If we further consider the patterns in Fig. 3(g) as crystal lattice, it would be a 2D oblique lattice with lattice constants $a_{\text{sample}} = 2.08$ nm, $b_{\text{sample}} = 3.71$ nm, both being much larger than (and incommensurate with) $a_{\text{Fe}(100)} = 0.286$ nm and $a_{\text{Fe}(110)} = 0.248$ nm.[69] One may speculate that the reason for such a lattice constant difference might be that the islands are products of iron–carbon compounds rather than pure Fe. However, if we focus on the graphene substrate at the border of an island, we can clearly resolve, as displayed in Fig. 4, that complete graphene lattice remains without any evidence of chemical reaction. Furthermore, when comparing the Wulff construction to our experimental results of the shapes of islands, the top facets can be identified as (110) and (100) surfaces of pristine bcc Fe crystal.

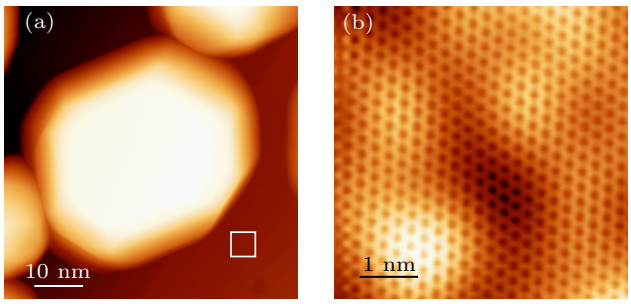


Fig. 4. STM images of Fe islands and graphene substrate after deposition at 873 K and annealing at 973 K for 15 min. (a) STM image of Fe islands and bare substrate in an 60 nm×60 nm area. (b) STM image taken directly on bare substrate close to an Fe island within the white square indicated in a, showing exactly the feature of graphene.

The crystal symmetry and lattice constant between bcc Fe and graphene is large. Consequently, the strain in the Fe islands should play an important role in the surface structures. For example, the study of Fe grown on W(110)[70,71] and Re (0001)[72] revealed that lattice mismatch between the Fe islands and the substrates easily leads to the formation of surface superstructures with stripes and/or nearly periodic dots. We thus attribute the observed patterns on our island tops in Figs. 3(c), 3(f) and 3(g) to the strain-induced surface superstructures. Our islands of measurement are about 60 ML in thickness and much thicker than the ones in Refs. [70–72], which may be the reason for the slightly different inter-stripe distances between them.

5. Summary

We have successfully prepared Fe islands on graphene by MBE. Through STM experiments, we found that the Fe islands have both flat and round tops, indicating that the growth of Fe islands is bimodal. We obtained the distribution of heights of the two modes and established that the Fe islands with flat tops have lower average height. On the flat-top islands, the orientations of the top facets were assigned according to the Wulff construction of bcc Fe. Our STM images of these facets revealed surface superstructure, which was presumably due to strain effects, although the mechanism of this phenomenon requires further theoretical study. Our successful preparation of Fe islands with well-defined shapes will facilitate the research of graphene-based spintronics.

Acknowledgements

We thank the Ministry of Science and Technology of China (Grant Nos. 2019YFA0308600 and 2020YFA0309000), the National Natural Science Foundation of China (Grant Nos. 92365302, 92065201, 22325203, 92265105, 12074247, and 12174252), the Strategic Priority Research Program of Chinese Academy of Sciences (Grant No. XDB28000000), and the Science and Technology Commission of Shanghai Municipality (Grant Nos. 2019SHZDZX01, 19JC1412701 and 20QA1405100) for financial support. We also acknowledge financial support from the Innovation Program for Quantum Science and Technology (Grant No. 2021ZD0302500).

References

[1] Novoselov K S, Geim A K, Morozov S V, Jiang D, Zhang Y, Dubonos S V., Grigorieva I V and Firsov A D 2004 *Science* **306** 666
[2] Geim A K and Novoselov K S 2007 *Nat. Mater.* **6** 183
[3] Peierls R 1935 *Ann. l'institut Henri Poincar* **5** 177
[4] Mermin N D 1968 *Phys. Rev.* **176** 250
[5] Wallace P R 1947 *Phys. Rev.* **71** 622
[6] McClure J W 1957 *Phys. Rev.* **108** 612
[7] Slonczewski J C and Weiss P R 1958 *Phys. Rev.* **109** 272
[8] Das Sarma S, Adam S, Hwang E H and Rossi E 2011 *Rev. Mod. Phys.* **83** 407
[9] Novoselov K S, Geim A K, Morozov S V, Jiang D, Katsnelson M I, Grigorieva I V, Dubonos S V and Firsov A A 2005 *Nature* **438** 197
[10] Zhang Y, Tan Y W, Stormer H L and Kim P 2005 *Nature* **438** 201
[11] Novoselov K S, Jiang Z, Zhang Y, Morozov S V, Stormer H L, Zeitler U, Maan J C, Boebinger G S, Kim P and Geim A K 2007 *Science* **315** 1379
[12] Castro Neto A H, Guinea F, Peres N M R, Novoselov K S and Geim A K 2009 *Rev. Mod. Phys.* **81** 109
[13] Chen G 2022 *Quantum Front.* **1** 8
[14] Liu Y W and He L 2023 *Quantum Front.* **2** 2
[15] Pathak S, Shenoy V B and Baskaran G 2010 *Phys. Rev. B* **81** 085431
[16] Nandkishore R, Levitov L S and Chubukov A V 2012 *Nat. Phys.* **8** 158
[17] Jiang S, Mesaros A and Ran Y 2014 *Phys. Rev. X* **4** 031040
[18] Ichinokura S, Sugawara K, Takayama A, Takahashi T and Hasegawa S 2016 *ACS Nano* **10** 2761
[19] Toyama H, Akiyama R, Ichinokura S, Hashizume M, Iimori T, Endo Y, Hobara R, Matsui T, Horii K, Sato S, Hirahara T, Komori F and Hasegawa S 2022 *ACS Nano* **16** 3582
[20] Wang X, Liu N, Wu Y, Qu Y, Zhang W, Wang J, Guan D, Wang S, Zheng H, Li Y, Liu C and Jia J 2022 *Nano Lett.* **22** 7651
[21] Sevinçli H, Topsakal M, Durgun E and Ciraci S 2008 *Phys. Rev. B* **77** 195434
[22] Uchoa B, Rappoport T G and Castro Neto A H 2011 *Phys. Rev. Lett.* **106** 016801
[23] Liu X, Han Y, Evans J W, Engstfeld A K, Behm R J, Tringides M C, Hupalo M, Lin H Q, Huang L, Ho K M, Appy D, Thiel P A and Wang C Z 2015 *Prog. Surf. Sci.* **90** 397
[24] Ren J, Guo H, Pan J, Zhang Y F, Yang Y, Wu X, Du S, Ouyang M and Gao H J 2017 *Phys. Rev. Lett.* **119** 176806
[25] Baltic R, Pivetta M, Donati F, Wäckerlin C, Singha A, Dreiser J, Rusponi S and Brune H 2016 *Nano Lett.* **16** 7610
[26] Ren J, Guo H, Pan J, Zhang Y F, Yang Y, Wu X, Du S, Ouyang M and Gao H J 2017 *Phys. Rev. Lett.* **119** 176806
[27] Gao M, Han X, Liu W, Tian Z, Mei Y, Zhang M, Chu P K, Kan E, Hu T, Du Y, Qiao S and Di Z 2021 *Sci. Adv.* **7** eabg7054

[28] Gyamfi M, Eelbo T, Waśniowska M and Wiesendanger R 2011 *Phys. Rev. B* **84** 113403
[29] Liu X, Wang C Z, Hupalo M, Lu W C, Thiel P A, Ho K M and Tringides M C 2011 *Phys. Rev. B* **84** 235446
[30] Liu X, Hupalo M, Wang C Z, Lu W C, Thiel P A, Ho K M and Tringides M C 2012 *Phys. Rev. B* **86** 081414
[31] Binz S M, Hupalo M, Liu X, Wang C Z, Lu W C, Thiel P A, Ho K M, Conrad E H and Tringides M C 2012 *Phys. Rev. Lett.* **109** 026103
[32] Liu X, Wang C Z, Lin H Q, Hupalo M, Thiel P A, Ho K M and Tringides M C 2014 *Phys. Rev. B* **90** 155444
[33] Liu W Q, Wang W Y, Wang J J, Wang F Q, Lu C, Jin F, Zhang A, Zhang Q M, Laan G Van Der, Xu Y B, Li Q X and Zhang R 2015 *Sci. Rep.* **5** 11911
[34] Zhu Y, Pan Y F, Yang Z Q, Wei X Y, Hu J, Feng Y P, Zhang H and Wu R Q 2019 *J. Phys. Chem. C* **123** 4441
[35] Kibria M T, Nakagawa T and Mizuno S 2020 *Appl. Surf. Sci.* **505** 144209
[36] Xu H K, Li F, Fei F C, Wang L, Gu Y S, Liu D, Yu Q Y, Xue S S, Peng K, Chen B, Xie H K, Zhu Z, Guan D D, Wang S Y, Li Y, Liu C, Song F, Zheng H and Jia J F 2022 *Quantum Front.* **1** 5
[37] Wang X, Chen C, Zhang T, Zhang T and Feng D 2022 *Quantum Front.* **1** 12
[38] Liu W, Hu Q, Wang X, Zhong Y, Yang F, Kong L, Cao L, Li G, Peng Y, Okazaki K, Kondo T, Jin C, Xu J, Gao H J and Ding H 2022 *Quantum Front.* **1** 20
[39] Wang Z, Liu L, Zhao M, Zheng H, Yang K, Wang C, Yang F, Wu H and Gao C 2022 *Quantum Front.* **1** 16
[40] Wang G Y, Xie W, Xu D, Ma H Y, Yang H, Lu H, Sun H H, Li Y Y, Jia S, Fu L, Zhang S and Jia J F 2019 *Nano Res.* **12** 569
[41] Yang B, Xia B, Chen H, Cai J, Yang H, Liu X, Liu L, Guan D, Wang S, Li Y, Zheng H, Liu C and Jia J 2023 *Adv. Quantum Technol.* **6** 2300137
[42] Wang M X, Liu C, Xu J P, Yang F, Miao L, Yao M Y, Gao C L, Shen C, Ma X, Chen X, Xu Z A, Liu Y, Zhang S C, Qian D, Jia J F and Xue Q K 2012 *Science* **335** 52
[43] Ge J F, Liu Z L, Liu C, Gao C L, Qian D, Xue Q K, Liu Y and Jia J F 2014 *Nat. Mater.* **14** 285
[44] Xu J P, Liu C, Wang M X, Ge J, Liu Z L, Yang X, Chen Y, Liu Y, Xu Z A, Gao C L, Qian D, Zhang F C and Jia J F 2014 *Phys. Rev. Lett.* **112** 217001
[45] Zhu F F, Chen W J, Xu Y, Gao C L, Guan D D, Liu C H, Qian D, Zhang S C and Jia J F 2015 *Nat. Mater.* **14** 1020
[46] Xu J P, Wang M X, Liu Z L, Ge J F, Yang X, Liu C, Xu Z A, Guan D, Gao C L, Qian D, Liu Y, Wang Q H, Zhang F C, Xue Q K and Jia J F 2015 *Phys. Rev. Lett.* **114** 017001
[47] Sun H H, Zhang K W, Hu L H, Li C, Wang G Y, Ma H Y, Xu Z A, Gao C L, Guan D D, Li Y Y, Liu C, Qian D, Zhou Y, Fu L, Li S C, Zhang F C and Jia J F 2016 *Phys. Rev. Lett.* **116** 257003
[48] Yang H, Li Y Y, Liu T T, Xue H Y, Guan D D, Wang S Y, Zheng H, Liu C H, Fu L, Jia J F, Yang H, Li Y, Liu T, Xue H, Guan D, Wang S, Zheng H, Liu C, Jia J and Fu L 2019 *Adv. Mater.* **31** 1905582
[49] Yao G, Duan M C, Liu N, Wu Y, Guan D D, Wang S, Zheng H, Li Y Y, Liu C and Jia J F 2019 *Phys. Rev. Lett.* **123** 257001
[50] Xue H Y, Yang H, Wu Y F, Yao G, Guan D D, Wang S Y, Zheng H, Liu C H, Li Y Y and Jia J F 2019 *Sci. China Physics, Mech. Astron.* **62** 76801
[51] Qin J, Zhao C, Xia B, Wang Z, Liu Y, Yang B, Guan D, Wang S, Li Y, Zheng H, Liu C and Jia J 2020 *Appl. Surf. Sci.* **512** 145644
[52] Qin J, Zhao C, Xia B, Wang Z, Liu Y, Guan D, Wang S, Li Y, Zheng H, Liu C and Jia J 2020 *Nanotechnology* **31** 305708
[53] Yang H, Li Y Y, Liu T T, Guan D D, Wang S Y, Zheng H, Liu C, Fu L and Jia J F 2020 *Phys. Rev. Lett.* **125** 136802
[54] Zhu Z, Papaj M, Nie X A, Xu H K, Gu Y S, Yang X, Guan D, Wang S, Li Y, Liu C, Luo J, Xu Z A, Zheng H, Fu L and Jia J F 2021 *Science* **374** 1381
[55] Zhao C, Li L, Zhang L, Qin J, Chen H, Xia B, Yang B, Zheng H, Wang S, Liu C, Li Y, Guan D, Cui P, Zhang Z and Jia J 2022 *Phys. Rev. Lett.* **128** 206802
[56] Zang Y, Zhu K, Li L and He K 2022 *Quantum Front.* **1** 11
[57] Zhang W, Wang X, Liu N, Wang J, Qu Y, Guan D D, Wang S, Zheng H, Li Y Y, Liu C and Jia J F 2023 *Appl. Surf. Sci.* **635** 157768
[58] Yang B, Zhao C, Xia B, Ma H, Chen H, Cai J, Yang H, Liu X, Liu L, Guan D, Wang S, Li Y, Liu C, Zheng H and Jia J 2023 *Quantum Front.* **2** 9
[59] Ding S, Zhao D, Jiang T, Wang H, Feng D and Zhang T 2023 *Quantum Front.* **2** 3
[60] Huang H, Shen J, Chen J, Shen Q, Lin G, Zhu Z, Wu J, Ma J, Yang H, Liu X, Liu L, Guan D, Wang S, Li Y, Liu C, Zheng H, Lu Y and Jia J 2023 *Quantum Front.* **2** 12
[61] Rahm J M and Erhart P 2020 *J. Open Source Softw.* **5** 1944
[62] Skriver H L and Rosengaard N M 1992 *Phys. Rev. B* **46** 7157
[63] Aldén M, Skriver H L, Mirbt S and Johansson B 1994 *Surf. Sci.* **315** 157
[64] Błoński P and Kiejna A 2004 *Vacuum* **74** 179
[65] Błoński P and Kiejna A 2007 *Surf. Sci.* **601** 123
[66] Vitos L, Ruban A V, Skriver H L and Kollár J 1998 *Surf. Sci.* **411** 186
[67] Kositski R and Mordehai D 2015 *Acta Mater.* **90** 370
[68] Tran R, Xu Z, Radhakrishnan B, Winston D, Sun W, Persson K A and Ong S P 2016 *Sci. Data* **3** 160080
[69] Jain A, Ong S P, Hautier G, Chen W, Richards W D, Dacek S, Cholia S, Gunter D, Skinner D, Ceder G and Persson K A 2013 *APL Mater.* **1** 011002
[70] Bethge H, Heuer D, Jensen C, Reshöft K and Köhler U 1995 *Surf. Sci.* **331–333** 878
[71] Bode M, Pascal R, Dreyer M and Wiesendanger R 1996 *Phys. Rev. B* **54** R8385
[72] Ouazi S, Pohlmann T, Kubetzka A, Von Bergmann K and Wiesendanger R 2014 *Surf. Sci.* **630** 280